Published in final edited form as:

Gut. 2018 May ; 67(5): 931–944. doi:10.1136/gutjnl-2017-314032.

Hepatoma-intrinsic CCRK inhibition diminishes myeloid-derived suppressor cell immunosuppression and enhances immune-checkpoint blockade efficacy

Jingying Zhou[1], **Man Liu**[1], **Hanyong Sun**[2], **Yu Feng**[1], **Liangliang Xu**[1], **Anthony W H Chan**[3], **Joanna H Tong**[3], **John Wong**[4], **Charing Ching Ning Chong**[4], **Paul B S Lai**[4], **Hector Kwong-Sang Wang**[5], **Shun-Wa Tsang**[5], **Tyler Goodwin**[6], **Rihe Liu**[6], **Leaf Huang**[6], **Zhiwei Chen**[7,8], **Joseph JY Sung**[2,9], **King Lau Chow**[5], **Ka Fai To**[3], and **Alfred Sze-Lok Cheng**[1,9]

[1]School of Biomedical Sciences, The Chinese University of Hong Kong, Hong Kong, China

[2]Department of Medicine and Therapeutics, The Chinese University of Hong Kong, Hong Kong, China

[3]Department of Anatomical and Cellular Pathology, The Chinese University of Hong Kong, Hong Kong, Hong Kong

[4]Department of Surgery, The Chinese University of Hong Kong, Hong Kong, Hong Kong

[5]Division of Life Science, Hong Kong University of Science and Technology, Hong Kong, Hong Kong

[6]Division of Pharmacoengineering and Molecular Pharmaceutics, Eshelman School of Pharmacy, University of North Carolina Chapel Hill, Chapel Hill, North Carolina, USA

[7]AIDS Institute, The University of Hong Kong, Hong Kong, Hong Kong

[8]Department of Microbiology and Research Center for Infection and Immunity, Li Ka Shing Faculty of Medicine, The University of Hong Kong, Hong Kong, Hong Kong

[9]State Key Laboratory of Digestive Disease, The Chinese University of Hong Kong, Hong Kong, Hong Kong

Abstract

Correspondence to: Professor Alfred Sze-Lok Cheng, School of Biomedical Sciences and State Key Laboratory of Digestive Disease, The Chinese University of Hong Kong, Shatin, Hong Kong, China; alfredcheng@cuhk.edu.hk.

Competing interests
None declared.

Patient consent
Parental/guardian consent obtained.

Ethics approval
Joint CUHK-NTEC Clinical Research Ethics Committee.

Provenance and peer review
Not commissioned; externally peer reviewed.

Contributors Study concept and design: JZ, AC ; acquisition of data: JZ, ML, HS, YF, LX, AWHC, JHT; analysis and interpretation of data: JZ, ML, HS, YF, AWHC, AC ; acquisition of patient specimens: AWHC, JW, CC, PL, KFT; drafting of the manuscript: JZ, AC ; critical revision of the manuscript: JZ, HW, TG, LH, KLC, AC ; obtained funding: JZ, RL, LH, JS, KLC, KFT, AC ; administrative, technical or other material support: HW, ST, TG, RL, LH, ZC, JS, KLC, KFT; study supervision: AC.

Objective—Myeloid-derived suppressor cells (MDSCs) contribute to tumour immunosuppressive microenvironment and immune-checkpoint blockade resistance. Emerging evidence highlights the pivotal functions of cyclin-dependent kinases (CDKs) in tumour immunity. Here we elucidated the role of tumour-intrinsic CDK20, or cell cycle-related kinase (CCRK) on immunosuppression in hepatocellular carcinoma (HCC).

Design—Immunosuppression of MDSCs derived from patients with HCC and relationship with CCRK were determined by flow cytometry, expression analyses and co-culture systems. Mechanistic studies were also conducted in liver-specific *CCRK*-inducible transgenic (TG) mice and Hepa1–6 orthotopic HCC models using CRISPR/Cas9-mediated *Ccrk* depletion and liver-targeted nanoparticles for interleukin (IL) 6 trapping. Tumorigenicity and immunophenotype were assessed on single or combined antiprogrammed death-1-ligand 1 (PD-L1) therapy.

Results—Tumour-infiltrating $CD11b^{+}CD33^{+}HLA\text{-}DR^{-}$ MDSCs from patients with HCC potently inhibited autologous $CD8^{+}$T cell proliferation. Concordant overexpression of CCRK and MDSC markers (CD11b/CD33) positively correlated with poorer survival rates. Hepatocellular CCRK stimulated immunosuppressive $CD11b^{+}CD33^{+}HLA\text{-}DR^{-}$ MDSC expansion from human peripheral blood mononuclear cells through upregulating IL-6. Mechanistically, CCRK activated nuclear factor-κB (NF-κB) via enhancer of zeste homolog 2 (EZH2) and facilitated NF-κB-EZH2 co-binding to *IL-6* promoter. Hepatic *CCRK* induction in TG mice activated the EZH2/NF-κB/IL-6 cascade, leading to accumulation of polymorphonuclear (PMN) MDSCs with potent T cell suppressive activity. In contrast, inhibiting tumorous *Ccrk* or hepatic IL-6 increased interferon γ^{+}tumour necrosis factor-$\alpha^{+}CD8^{+}$ T cell infiltration and impaired tumorigenicity, which was rescued by restoring PMN-MDSCs. Notably, tumorous *Ccrk* depletion upregulated PD-L1 expression and increased intratumorous $CD8^{+}$ T cells, thus enhancing PD-L1 blockade efficacy to eradicate HCC.

Conclusion—Our results delineate an immunosuppressive mechanism of the hepatoma-intrinsic CCRK signalling and highlight an overexpressed kinase target whose inhibition might empower HCC immunotherapy.

INTRODUCTION

Hepatocellular carcinoma (HCC) is the second leading cause of cancer-related deaths worldwide. While chronic hepatitis B/C virus infections account for more than 80% of the HCCs in eastern Asia and sub-Saharan Africa,[1] non-alcoholic fatty liver disease (NAFLD) has become the major predisposing factor in Western countries, whose HCC incidence rises dramatically in parallel with the obesity and diabetes epidemics.[2] Both viral and NAFLD-associated HCCs are characterised by strong sexual dimorphism, with male-to-female ratio ranging from 2:1 to 7:1.[12] Despite the advancement in molecular therapy using the multikinase inhibitor sorafenib, the prognosis of advanced HCCs remains poor, with 5-year survival rates of 3%–11%.[3] Taken together with the recent failure of multiple phase III clinical trials of targeted therapies and the lack of druggable driver mutations as revealed by the HCC genomics studies,[3] contemporary clinical investigations have geared towards cancer immunotherapy which harnesses the patient's own T cell activity. Therapeutic blockade of T cell co-inhibitory molecules including cytotoxic T-lymphocyte associated protein 4 (CTLA-4), programmed cell death receptor 1 (PD-1) or its ligand (PD-L1) has

demonstrated durable antitumour responses and long-term remissions in a subset of patients with many solid and haematological cancers.[4–6] While the current HCC immunotherapy trials have produced favourable results, the relatively low response rates emphasise the strong immunosuppressive barriers which need to be tackled by complementary immune-stimulatory approaches.[7–9]

Cancer cells and tumour-associated suppressive cells can alter the intratumorous T cell landscape through production of multiple immunosuppressive metabolites/cytokines and expression of checkpoint molecules such as PD-L1 which induce T cell exhaustion.[10] These T cell-inhibitory mechanisms are activated in the tumour microenvironment of a broad spectrum of cancers including HCC, which is often characterised by 'exhausted' $CD8^+$ T cells with high PD-1 expression.[1112] Growing evidence suggests that sufficient tumour-infiltrating $CD8^+$ T cells and PD-L1 expression are associated with clinical responses to PD-L1 blockade.[561314] Therefore, delineating the molecular mechanisms underlying T cell dysfunction in HCC is instrumental for developing novel combination strategies that can improve the responsiveness to immunotherapy.

Myeloid-derived suppressor cells (MDSCs) represent the major immunosuppressive population that exists only in pathological conditions such as chronic inflammation and cancer.[15] The tumour microenvironment secretes many different cytokines and chemokines to promote the generation and egress of these immature myeloid cells from the bone marrow (BM) into the tumour sites, which in turn suppress $CD8^+$ T cell proliferation and function by depriving amino acids via arginase-I expression, releasing oxidising molecules, and inducing other immunosuppressive cells such as tumour-associated macrophages and regulatory T cells.[15] Human MDSCs are phenotypically characterised as $CD11b^+$, $CD33^+$, $HLA\text{-}DR^-$, and can be divided into granulocytic ($CD14^-/CD15^+/CD66b^+$) and monocytic ($CD14^+$) subtypes.[16] In patients with HCC, both $CD14^-$[17] and $CD14^+$ MDSCs[18] have been shown to accumulate in the peripheral blood or tumour tissues, and associate with poor prognosis.[1920] However, little is known about the phenotypes of MDSCs within the human HCC microenvironment. More importantly, despite the insight provided by different murine models,[21] the tumour-intrinsic oncogenic signalling that drives MDSC accumulation and activation in human HCCs remains poorly defined.

Given their pivotal roles in cell cycle and transcriptional regulation, deregulation of cyclin-dependent kinases (CDKs) has become a hallmark of several cancer types.[22] Accordingly, pharmacological inhibition of some of these serine/threonine kinases has produced promising results in clinical trials.[2324] We have recently uncovered the role of the latest family member CDK20 or cell cycle-related kinase (CCRK) in driving hepatocarcinogenesis in men.[25–27] Upregulated by aberrant androgen receptor (AR) signalling in either viral or NAFLD condition, CCRK functions as a signalling hub to connect multiple oncogenic transcriptional regulators such as β-catenin/T cell factor and enhancer of zeste homologue 2 (EZH2), as well as kinases such as glycogen synthase kinase 3β (GSK-3β) and protein kinase B (AKT).[25–27] As emerging evidence highlights the key roles of CDKs in tumour immunity,[2829] we aimed to explore the immunomodulatory function of CCRK in human HCC. Here we provide evidence from clinical specimens, co-culture systems, liver-specific *CCRK*-inducible transgenic (TG) mice and orthotopic HCC models to illustrate a hepatoma-

intrinsic CCRK-interleukin(IL) 6 pathway that renders T cell dysfunction via MDSC-mediated immunosuppression. As we also found that tumorous *Ccrk* depletion significantly enhanced PD-L1 blockade efficacy in the preclinical model, our study suggests a new kinase target to improve HCC immunotherapy.

METHODS

Patient samples

Paired tumour and non-tumour tissues from 162 patients with HCC who underwent liver resection at the Prince of Wales Hospital (Hong Kong) were collected for immune profiling, quantitative reverse transcription-PCR (qRT-PCR) and immunohistochemical analyses (see supplementary methods for details). Eight histologically normal livers from patients with benign focal nodular hyperplasia and 12 blood samples from healthy subjects served as controls. Studies using human specimen were approved by the joint CUHK-NTEC Clinical Research Ethics Committee.

Cell culture and transfection

Huh7, PLC5 and Sk-Hep1 HCC cell lines and the immortal human liver cell line LO2 were transfected with wild type (WT)/kinase-defective (KD) CCRK-expressing or pcDNA3.1 control vector as well as different short-interfering RNAs (siRNAs), followed by gene expression, co-immunoprecipitation and quantitative chromatin immunoprecipitation-PCR (qChIP-PCR) analyses as previously described.[25–27]

MDSC and T cell proliferation assays

Single cells freshly isolated from human blood, liver and tumour tissues were analysed for MDSC phenotypes and autologous T cell proliferation by flow cytometry using FACSFusion (BD Biosciences).[30] Human peripheral blood mononuclear cells (PBMCs) freshly isolated from buffy coats of anonymous healthy donors were treated by supernatants of transfected cells for 5 days and then analysed for MDSC expansion and T cell suppression (see supplementary methods).

Liver-specific CCRK-inducible TG mouse model

The liver-specific *CCRK*-inducible TG mouse model was constructed as described in supplementary methods. At 10-day and 4-week post-tamoxifen injection, the transgene expression and myeloid cell proportions and functions were analysed by western blot and flow cytometry, respectively.[30]

Orthotopic HCC models and liver-targeted nanoparticles

An orthotopic HCC model was established as described in supplementary methods using a luciferase-stably transfected mouse hepatoma cell line Hepa1–6,[31] in which *Ccrk* knockout (CrCcrk) or control (CrCtrl) cells were generated by clustered regularly interspaced short palindromic repeats (CRISPR)/Cas9 and confirmed by sequencing and western blot. Orthotopic tumour-bearing mice were treated by BM-derived polymorphonuclear (PMN)-MDSCs from naïve CAG-DsRed fluorescence protein (RFP) TG mouse or lipid/calcium/

phosphate nanoparticles optimised for delivering plasmid DNA encoding an IL-6 protein trap (pIL-6-trap) or green fluorescent protein control (pGFP)[32] as described in supplementary methods. In addition, a large hepatoma model was established by injection of 5×10^6 cells into the liver capsule. CrCtrl or CrCcrk tumour-bearing mice were treated with PD-L1 blockade antibody (10F.9G2, Bio-X-Cell) or rat IgG2b control (LTF-2, Bio-X-Cell) via intraperitoneal injection (200 μg/each), followed by tumorigenicity and immunophenotypical assessments.[33]

Statistical analysis

The independent Student's t-test was used to compare data between two groups. The clinicopathological features of patients with HCC with high or low *CD11b*/*CD33*/*CCRK*/*IL-6* expressions were compared using Fisher's exact test for categorical variables and Mann-Whitney U test for continuous data.[25] The Kaplan-Meier survival analysis was also performed. A two-tailed p value <0.05 was considered statistically significant.

RESULTS

Tumour-infiltrating CD11b$^+$CD33$^+$HLA-DR$^-$ MDSCs in patients with HCC exert potent autologous CD8$^+$ T cell suppression

We first investigated the abundance of CD11b$^+$CD33$^+$HLA-DR$^-$ immature myeloid cells in patients with HCC by fluorescence-activated cell sorting (FACS), which contained similar levels of both monocytic (CD14$^+$) and granulocytic (CD15$^+$) subsets[16] (online supplementary figure 1A, B), and observed significantly higher frequencies in tumours, matched non-tumour liver tissues and PBMCs compared with PMBCs of healthy donors ($p<0.05$; figure 1A). While there was no obvious difference in CD14$^+$ monocytic (M)-MDSCs between genders, we observed a trend of higher CD15$^+$ granulocytic MDSCs in blood, non-tumour and tumour tissues in male compared with female patients (online supplementary figure 1C,D). In contrast, the frequencies of CD8$^+$ T cells in tumours, livers and PBMCs of patients with HCC were significantly lower than the PMBCs of healthy donors ($p<0.01$; figure 1B). We next performed immunohistochemistry for CD8 and the myeloid cell marker CD11b in human HCC tissues (figure 1C and online supplementary figure 1E). Interestingly, the intratumorous CD8 immunohistochemical score was positively correlated with CD11b in 33 patients with HCC ($p<0.0001$; figure 1C), indicating that the intratumorous CD8$^+$ T cells may be inactivated in the tumour microenvironment[12] (data not shown). We further performed autologous CD8$^+$ T cell proliferation assay to investigate the immunosuppressive activity of the CD11b$^+$CD33$^+$HLA-DR$^-$ cells derived from patients with HCC and observed potent inhibition of CD3/CD28-induced and IL-2-induced T cell proliferation, in particular by co-cultured CD11b$^+$CD33$^+$HLA-DR$^-$ cells from tumour of patients with HCC (figure 1D), thus verifying their MDSC identity.[16]

Concordant overexpression of CCRK and MDSC markers in HCCs correlates with poor prognosis of patients

Given the strong oncogenic activity of CCRK in HCC,[25–27] we next investigated the relationship between CCRK and MDSCs in clinical samples by qRT-PCR using 8 normal livers and 122 pairs of HCC tumour and non-tumour liver tissues. In contrast to the low

basal levels in normal livers, upregulation of *CD11b*, *CD33* and *CCRK* expressions were observed in human HCCs (figure 1E). Association analyses showed that while the MDSC markers *CD11b* and *CD33* positively and significantly correlated with each other ($p<0.0001$), their expressions also significantly correlated with *CCRK* ($p<0.0001$; figure 1E), which could be observed in both genders (online supplementary figure 2A). Consistent with our previous observation, the *CCRK* transcript and protein levels in tumour tissues were significantly higher than those in non-tumour tissues in male but not female patients (online supplementary figure 2B). We further investigated whether overexpression of *CCRK* and MDSC markers associates with prognosis of 102 patients with HCC which were supplemented with clinicopathological and survival data. Kaplan-Meier analysis revealed that patients with HCC with high *CD11b*/*CD33*/*CCRK* expressions significantly correlated with shorter overall (HR=2.813; $p<0.05$; figure 1F) and disease-free survival rates (HR=2.011; $p<0.05$; figure 1G). We confirmed the prognostic associations using an independent cohort of 34 patients with HCC with semiquantitative CD11b and CCRK protein levels by immunohistochemistry and western blot,[27] respectively (online supplementary figure 2C), thus demonstrating the clinical significance of concordant CCRK overexpression and MDSC accumulation in HCC.

Hepatocellular CCRK stimulates MDSC expansion from human PBMCs

We next determined whether CCRK induces the accumulation of MDSCs that share the same phenotypes of the MDSCs derived from patients with HCC using human PBMCs (online supplementary figure 3A). Conditional medium of LO2 hepatocytes or Sk-Hep1 HCC cells on ectopic expression of WT CCRK, but not the KD mutant[2627] (figure 2A), significantly induced the expansion of $CD11b^{+}CD33^{+}HLA\text{-}DR^{-}$ MDSCs from PBMCs ($p<0.05$; figure 2B), which was accompanied by increased T cell-suppressive function as shown by reduced T cell proliferation ($p<0.05$; figure 2C and online supplementary figure 3B) and interferon γ (IFN-γ) production ($p<0.05$; figure 2D). In the complementary experiments, PBMCs cultured with conditional medium of Huh7 or PLC5 HCC cells on siRNA-mediated knockdown of CCRK (figure 2E) resulted in a significantly lower population of MDSCs ($p<0.05$; figure 2F), which exhibited lower T cell-suppressive activities (figure 2G,H). Taken together, these findings suggest that hepatocellular CCRK expression induces the accumulation of MDSCs with T cell-immunosuppressive activity.

Hepatocellular CCRK drives MDSC accumulation through IL-6 production

To identify the factor(s) in the conditional medium of CCRK-expressing hepatocytes/HCC cells that mediates MDSC accumulation, we measured the gene expression levels of 27 cytokines and chemokines in transfected cells by qRT-PCR (online supplementary table 1). Compared with control, ectopic WT CCRK expression significantly induced the expressions of *IL-1β*, *IL-6*, *tumour necrosis factor-α (TNF-α)*, *IFN-β*, *C-C motif chemokine ligand 2 (CCL2)* and *CCL4* in both LO2 and Sk-Hep1 cells ($p<0.05$; figure 3A and online supplementary figure 4). While the CCRK-induced chemokines may influence MDSC recruitment, we selectively confirmed the significant secretion of IL-6 in LO2 and Sk-Hep1 cells expressing WT but not KD CCRK ($p<0.05$; figure 3B), since this proinflammatory cytokine, in combination with granulocyte-macrophage colony-stimulating factor, has been shown to induce the generation of MDSCs with the most potent T cell suppressive capacity.

[15] To determine the importance of IL-6 in hepatocellular CCRK-induced MDSC accumulation, IL-6 neutralisation antibody (Nab) or isotype control was added into the conditional media of CCRK-expressing LO2 and Sk-Hep1 cells. The results showed that IL-6 Nab completely abolished the CCRK-induced MDSC expansion from PBMCs ($p<0.05$; figure 3C) and the consequential T cell inhibition ($p<0.05$; figure 3D). In the reciprocal experiments, knockdown of CCRK dramatically reduced IL-6 expression and secretion in Huh7 and PLC5 HCC cells ($p<0.05$; figure 3E,F). Notably, addition of IL-6 recombinant protein in the conditional medium of CCRK-knockdown cells fully restored the MDSC induction ($p<0.05$; figure 3G) and T cell inhibition ($p<0.05$; figure 3H). In support of the notion that hepatocellular CCRK induces MDSC accumulation and functions via IL-6 production, significant correlations among *CCRK*, *IL-6*, *CD11b* and *CD33* expressions were detected in human HCCs ($p<0.0001$; figure 3I–K). Serum IL-6 concentrations were also significantly higher in patients with HCC than healthy donors ($p<0.01$; figure 3L). Clinicopathological correlation analysis demonstrated that patients with HCC with high *CCRK/IL-6/CD11b*/*CD33* expressions were significantly associated with hepatitis virus infection ($p<0.05$; online supplementary table 2). Moreover, Kaplan-Meier analysis also showed the worse prognostic association of concordant upregulation of these genes in patients with HCC ($p<0.05$; online supplementary figure 2D). These data indicate that the CCRK/IL-6 signalling contributes to MDSC accumulation which negatively impacts the survival of patients with HCC.

CCRK upregulates IL-6 through EZH2/NF-κB signalling

We next elucidated the molecular mechanism underlying CCRK-induced IL-6 production. We speculated that CCRK may activate nuclear factor-κB (NF-κB) signalling due to the concordant upregulation of NF-κB responsive genes (*IL-1β*, *IL-6*, *TNF-α*, *CCL2*) by CCRK (online supplementary figure 4). Indeed, ectopic expression of WT but not KD CCRK in LO2 and Sk-Hep1 cells increased the phosphorylation of p65 at Ser536 (p-p65^{Ser536}), while the basal levels of p50 and p65 did not change (figure 4A). To investigate the role of NF-κB in CCRK-induced IL-6 production, we treated both LO2 and Sk-Hep1 lines with JSH-23 which interferes with NF-κB nuclear translocation.[34] JSH-23 abrogated both CCRK-induced *IL-6* expression and production ($p<0.05$; figure 4B).

As CCRK drives hepatocarcinogenesis through upregulation of EZH2,[27] which can function as a transcriptional activator of NF-κB targets,[35] we determined whether CCRK activates NF-κB/IL-6 signalling through EZH2. Knockdown of EZH2 by siRNA in LO2 and Sk-Hep1 cells abrogated CCRK-induced p-p65^{Ser536} (figure 4C), and *IL-6* expression and production (figure 4D). Conversely, knockdown of CCRK in Huh7 and PLC5 cells decreased p-p65^{Ser536} (figure 4E) and IL-6 levels (figure 4F), which could be rescued by ectopic EZH2 expression (figure 4E,F). Since the transactivating function of EZH2 is independent of its histone methyltransferase activity but requires the physical interaction with NF-κB,[35] we next conducted co-immunoprecipitation and qChIP-PCR assays to determine whether EZH2 physically interacts with p-p65^{Ser536} to facilitate CCRK-induced *IL-6* expression. We found that CCRK overexpression induced a robust EZH2-p-p65^{Ser536} complex formation (figure 4G) and co-occupancy of *IL-6* promoter (figure 4H). Concordant CCRK, EZH2 and p-

p65^{Ser536} overexpression in human HCCs (figure 4I) further supports the notion that CCRK upregulates *IL-6* expression and production in an EZH2/NF-κB-dependent manner.

Liver-specific CCRK TG mice exhibit Ezh2/NF-κB/IL-6 activation and immunosuppressive MDSC accumulation

To investigate the effects of CCRK on IL-6 production and MDSC accumulation in vivo, we have established a TG mouse model that specifically expresses human *CCRK* in a tissue-specific and temporal-specific manner. The transgene expression was controlled by a liver-specific *transferrin* promoter (*pTf*) in a tamoxifen-inducible setting (online supplementary figure 5A). At 10 days post-tamoxifen stimulation, *CCRK* expression was induced in the liver of *pTf-LSL-CCRK/+; Rosa26CreERt2/+* TG mouse compared with *Rosa26CreERt2/+* control mouse (figure 5A). Consistent with the in vitro findings, the hepatic Ezh2 and p-p65^{Ser536} expression (figure 5A) as well as the hepatocellular (figure 5B) and serum IL-6 levels (figure 5C) were upregulated. Using TG mouse-derived primary cells, we confirmed that the Ezh2-NF-κB cascade was activated in the hepatocytes (figure 5D).

We next examined the myeloid cell populations in the blood and liver of control and *CCRK* TG mice at 1 month post-tamoxifen injection via phenotypical profiling of M-MDSC (CD11b$^+$Gr-1$^+$Ly6G$^-$Ly6C$^+$), PMN-MDSC (CD11b$^+$Gr-1$^+$Ly6G$^+$Ly6C^{int}) and macrophage (CD11b$^+$Gr-1$^-$F4/80$^+$Ly6C$^-$) (online supplementary figure 5B).[16] FACS analysis demonstrated a significant induction of circulating MDSCs in *CCRK* TG mice compared with control mice (figure 5E). The enriched MDSCs mainly presented PMN-MDSC phenotype with high Ly6G and intermediate Ly6C expressions ($p<0.01$; figure 5E,F), which remained elevated for at least 90 days after tamoxifen stimulation (online supplementary figure 5C). Consistent with the observations in patients with HCC, we observed a significant increase in the circulating PMN-MDSCs, but not M-MDSCs, in male compared with female CCRK TG mice at 1 month post-tamoxifen stimulation (online supplementary figure 5D). In contrast, other CD11b$^+$ myeloid populations did not show significant differences (figure 5F). Notably, liver-infiltrating PMN-MDSCs were also enriched in *CCRK* TG mice compared with control mice (figure 5G,H). To determine whether the CD11b$^+$Gr-1$^+$Ly6G$^+$Ly6C^{int} PMN-MDSCs possess immunosuppressive function, the same number of PMN-MDSCs from the blood or liver of TG and control mice were co-cultured with allogeneic splenic T cells. We found that the blood PMN-MDSCs from the TG mice exerted a strong inhibition of T cell proliferation compared with those of the control mice (figure 5I). Notably, the liver-infiltrating PMN-MDSCs from TG mice exhibited even more potent T cell suppression (figure 5J). These data support the notion that hepatocellular CCRK activates EZH2/NF-κB/IL-6 signalling to specifically induce accumulation of immunosuppressive PMN-MDSCs in the liver.

Ccrk-IL-6 signalling drives liver tumorigenicity through MDSC immunosuppression

Since CCRK induces MDSC accumulation in vitro (figure 2) and in vivo (figure 5), we next investigated the role of MDSCs in CCRK-induced hepatocarcinogenesis using an orthotopic model via syngeneic Hepa1-6 HCC cells in C57BL/6 immune-competent mice[31] (online supplementary figure 6A). BM-derived RFP$^+$PMN-MDSCs were generated (online supplementary figure 6B) for adoptive transfers in a 5-day interval based on their survival in

blood and tumour tissues on tail vein injection (online supplementary figure 6C). CRISPR/Cas9-mediated depletion of *Ccrk* (CrCcrk) in Hepa1–6 cells diminished the Ccrk/Ezh2/p-p65^{Ser536}signalling cascade (figure 6A) as well as IL-6 production in vitro ($p<0.05$; figure 6B) and in vivo ($p<0.01$; figure 6C) as compared with the control CrCtrl cells. *Ccrk* depletion significantly attenuated liver tumorigenicity by 60% ($p<0.001$; figure 6D), which was accompanied by reduced circulating, liver and tumour-infiltrating levels of CD11b^{+}Gr-1^{+}Ly6G^{+}Ly-6C^{int} PMN-MDSCs ($p<0.05$; figure 6E and online supplementary figure 6D) and increased IFN-γ^{+} TNF-α^{+}CD8^{+} T cells ($p<0.05$; figure 6F and online supplementary figure 6E). Notably, restoration of IL-6-expressing and Arg-I-expressing PMN-MDSCs (figure 6E, online supplementary figure 6F,G) by adoptive transfers abrogated the tumorous infiltration of IFN-γ^{+} TNF-α^{+}CD8^{+} T cells ($p<0.05$; figure 6F), leading to a complete rescue of the CrCcrk tumorigenicity ($p<0.001$; figure 6D). These findings demonstrate that MDSCs play an important role in CCRK-induced T cell dysfunction and hepatocarcinogenesis.

To elucidate the immunomodulatory and oncogenic role of IL-6 in vivo, we diminished the hepatic IL-6 levels via nanoparticle-mediated delivery of plasmid DNA encoding an engineered pIL-6-trap to the nucleus of liver hepatocytes[32] (online supplementary figure 7A). Repeated pIL-6-trap administration in the orthotopic HCC model significantly reduced the hepatic IL-6 protein levels by 50% when compared with the pGFP control ($p<0.001$; figure 6G), which dramatically inhibited HCC growth by 85% as determined by the luminescence intensity ($p<0.01$; figure 6H). Concurrently, pIL-6-trap significantly reduced the tumour-infiltrating IL-6^{+}Arg-I^{+} PMN-MDSCs ($p<0.01$; figure 6I and online supplementary figure 7B) and elevated the IFN-γ^{+} TNF-α^{+}CD8^{+} T cells ($p<0.001$; figure 6J). The same immunophenotype was also observed in the liver (online supplementary figure 7C) but not blood (online supplementary figure 7D) of the treated mice. Notably, while pIL-6-trap administration did not influence tumour cell proliferation as measured by intracellular Ki67 staining (online supplementary figure 7E), necrotic tumour cells were significantly increased ($p<0.05$; online supplementary figure 7F), presumably triggered by the elevated cytotoxic CD8^{+} T cells. These data suggest that local blockade of IL-6 attenuates HCC growth at least partially through inhibiting MDSC immunosuppression in the tumour microenvironment.

Combined blockade of Ccrk and PD-L1 eradicates large hepatoma

Finally, we determined the therapeutic potential of CCRK inhibition using a large hepatoma model via direct intrahepatic injection of Hepa1-6 cells into the liver capsule (figure 7A). As expected, *Ccrk* depletion significantly reduced the tumorous IL-6 protein level in CrCcrk tumours as compared with the CrCtrl tumours ($p<0.001$; figure 7B,C). Intriguingly, CrCcrk tumours exhibited significantly higher PD-L1 level ($p<0.001$; figure 7D,E) in conjunction to a significant increase in tumour-infiltrating CD8^{+} T cells ($p<0.001$; figure 7F). While the *PD-L1* transcript level was significantly higher in human HCCs compared with non-tumour tissues, no significant difference in *PD-L1* expression between high- and low-*CCRK*-expressing HCCs was observed (online supplementary figure 8A). Since high intratumorous CD8^{+} T cell level, tumorous PD-L1 expression and low MDSC level are immunogenic biomarkers indicating potential response from PD-1/PD-L1 pathway blockade,[4–6][13][14] we

combinatorially modulated both *Ccrk* and PD-L1 by administering PD-L1 blockade antibody (10F.9G2) or the control rat IgG2b (LTF-2) into CrCtrl or CrCcrk tumour-bearing mice (figure 7G). Although either *Ccrk* depletion or 10F.9G2 treatment significantly reduced tumorigenicity as compared with isotype/genotype control in LTF-2-treated CrCtrl tumour-bearing mice ($p<0.05$ or $p<0.01$, respectively), these single treatments alone were unable to eradicate the large hepatoma (figure 7H). Notably, co-blockade of *Ccrk* and PD-L1 markedly improved the treatment, curing 40% (4/10) of the 10F.9G2-treated CrCcrk tumour-bearing mice ($p<0.01$; figure 7H). FACS analysis revealed significant reduction in the percentages of tumour-infiltrating PMN-MDSCs and M-MDSCs from mice receiving the co-blockade ($p<0.001$ and $p<0.05$, respectively; figure 7I), which were accompanied by markedly increased cytotoxic IFN-γ^+ TNF-α^+CD8$^+$ T cells ($p<0.01$; figure 7J). Moreover, a similar immunophenotype pattern was observed in the liver of the co-blockade-treated mice (online supplementary figure 8B–D). These findings demonstrate that targeted inhibition of *Ccrk* enhances the efficacy of anti-PD-L1 in HCC via abrogation of MDSC immunosuppression.

DISCUSSION

Accumulating evidence from preclinical and clinical studies suggests that the tumour microenvironment, especially the immunosuppressive myeloid cells,[36–38] represents the Achilles' heel of cancer immunotherapy.[4–6] As MDSCs have emerged as a major barrier of antitumour immunity in human HCCs,[17–20] understanding the mechanisms of MDSC accumulation and functions will guide rational design of combination therapies. Here we report a hepatocellular CCRK/EZH2/NF-κB/IL-6 signalling that mitigates antitumour T cell responses by induction of MDSC immunosuppression. Corroborating evidence from the liver-specific *CCRK* TG model revealed a specific expansion and recruitment of PMN-MDSCs with potent T cell-suppressive activity. Functional analyses by genome editing, liver-targeted nanoparticle and adoptive transfer in orthotopic HCC model further showed that inhibiting the hepatoma Ccrk-IL-6 signalling circumvents MDSC-mediated IFN-γ^+ TNF-α^+CD8$^+$ T cell exhaustion, leading to a dramatic reduction in tumorigenicity. More importantly, tumorous *Ccrk* depletion improves the efficacy of anti-PD-L1 therapy to unleash greater cytotoxic T cell responses for large hepatoma eradication. Taken together, our results underscore an instrumental role of tumour-intrinsic CCRK signalling in fostering HCC immune evasion (figure 8).

The androgen/AR-activated CCRK signalling has been regarded as a key pathway contributing to the male predominance of human HCC.[3940] In this study, we have discovered a non-cell-autonomous protumorigenic function of CCRK in driving the expansion of MDSCs via NF-κB-mediated production of IL-6. This tumour-promoting cytokine, which could also be produced by the liver-resident macrophages, Kupffer cells, during acute liver damage and inflammation,[41] is crucial for hepatocellular proliferation and malignant progression.[42] Interestingly, oestrogen levels in female mice could effectively suppress NF-κB-dependent IL-6 production from Kupffer cells, thus inhibiting chemically induced hepatocarcinogenesis.[43] These findings unveil a complex interplay between sex hormone signalling and innate immune system during HCC development, which would need further investigation into the gender difference of immunity.[244] In addition, we found that majority

of the liver-infiltrating and tumour-infiltrating MDSCs produced IL-6, which may promote further MDSC accumulation, and feed back induced tumour cell-intrinsic CCRK signalling via signal transducer and activator of transcription 3 activation to form a vicious cycle (data not shown). Liver-specific IL-6 trapping in our orthotopic HCC model dramatically diminished tumorigenicity partially via reduced MDSC immunosuppression and increased cytotoxic $CD8^+$ T cell activity, further highlighting the importance of CCRK/IL-6 signalling in the immune regulation of hepatocarcinogenesis.

Our group has previously reported that dual GSK-3β and AKT phosphorylation by CCRK regulates the transcription and phosphorylation of EZH2,[27] which in turn upregulates a β-catenin/AR cascade to transactivate *CCRK*[2526] to constitute a vicious epigenetic circuitry in HCC.[27] In addition to CCRK, at least three components of this circuitry have been recently shown to exert tumour-immune escape functions. First, melanoma-cell-intrinsic β-catenin signalling contributes to T cell exclusion from tumour microenvironment via suppression of dendritic cell (DC) recruitment.[45] Besides, EZH2-mediated epigenetic silencing of T helper 1-type chemokines, *CXCL9* and *CXCL10*, restrains intratumorous effector T cell infiltration to enhance ovarian cancer progression.[46] More recently, the AKT-mechanistic target of rapamycin signalling has been shown to drive granulocytic MDSC accumulation to promote mammary carcinogenesis.[47] Taken together, these findings suggest that the self-reinforcing CCRK circuitry may orchestrate the establishment of immunosuppressive tumour microenvironment by enriching protumorigenic MDSCs and excluding antitumour DCs and effector T cells. This notion is supported by the marked increase in intratumorous IFN-γ^+TNF-α^+CD8^+ T cell infiltration in *Ccrk*-depleted tumours, which provides proof of concept for the development of CCRK inhibitors to overcome tumour-mediated immunosuppression.

Immunotherapy targeting the immune checkpoint inhibitors has been approved for the treatment of an expanding list of cancers.[4–6] Clinical trials of PD-L1/PD-1 antibodies in HCC have also shown favourable results,[7–9] however, the response rates (~20%) appear to be much lower than that of the immunogenic tumours such as melanoma and Hodgkin's lymphoma (~40%–90%), which are characterised by higher tumorous PD-L1 expression, intratumorous $CD8^+$ T cell level, and less immunosuppressive microenvironment in most responding patients.[4–6] These clinical observations underscore the compelling need to reverse the non-immunogenic liver tumour microenvironment for better therapeutic responses to checkpoint therapy. Notably, we found that tumorous *Ccrk* depletion increased PD-L1 expression, intratumorous effector T cells and reduced MDSC immunosuppression, thus presumably rendering the tumour more susceptible to PD-L1 blockade.[4–61314] Indeed, data from our preclinical HCC model showed that co-blockade of *Ccrk* and PD-L1 engendered potent IFN-γ^+TNF-α^+CD8^+ T cell responses to induce complete remission in 40% of the tumour-bearing mice. The mechanism underlying PD-L1 upregulation in *Ccrk*-depleted hepatoma is currently unknown. One possibility is that the activated T cells release type I and type II IFN to stimulate de novo PD-L1 expression,[45] which will need further elucidation.

Our clinical data demonstrated that $CD11b^+CD33^+$HLA-DR^- MDSCs are elevated in both peripheral blood and intratumorous tissues of patients with HCC and potently inhibit $CD8^+$ T cell proliferation. Moreover, concordant overexpression of CCRK and T cell-suppressive

MDSC markers is significantly associated with poorer patient survival. Nevertheless, the current study is limited by the availability of fresh patient samples for immune profiling. More clinical samples, especially female HCCs, will be required to elucidate whether CCRK-mediated MDSC expansion and recruitment is similar among the genders. Elevated circulating levels of $CD11b^{+}CD33^{+}HLA\text{-}DR^{-}$ MDSCs in patients with advanced melanoma have been shown to significantly correlate with poor responsiveness to anti-CTLA4 therapy.[48] Besides its predictive value for treatment response, these findings further vindicate the therapeutic potential of targeting MDSC to empower cancer immunotherapy.[36–38] Taken together with the multiple facets of CCRK in promoting hepatic carcinogenesis[25–27] and the rapid development of selective CDK inhibitors for cancer therapy,[2324] this study provides the rationale for targeting the druggable CCRK to augment immunotherapy of HCC.

Supplementary Material

Refer to Web version on PubMed Central for supplementary material.

Acknowledgments

Funding

This project is supported by the University Grants Committee through the Collaborative Research Fund C4017-14G, General Research Fund 14120816 and 14102914, the Food and Health Bureau through Heath and Medical Research Fund 03141376, and the Focused Innovations Scheme B 1907309 from the Chinese University of Hong Kong (CUHK). Alfred S.L Cheng is supported by funding from the Young Researcher Award, CUHK. Work at UNC is supported by grants from the National Institute of Health (DK100664, CA198999 and CA157738).

References

1. El-Serag HB. Epidemiology of viral hepatitis and hepatocellular carcinoma. Gastroenterology. 2012; 142:1264–73. [PubMed: 22537432]
2. Cheung OK, Cheng AS. Gender differences in Adipocyte Metabolism and liver cancer progression. Front Genet. 2016; 7:168. [PubMed: 27703473]
3. Llovet JM, Villanueva A, Lachenmayer A, et al. Advances in targeted therapies for hepatocellular carcinoma in the genomic era. Nat Rev Clin Oncol. 2015; 12:436.
4. Sharma P, Allison JP. The future of immune checkpoint therapy. Science. 2015; 348:56–61. [PubMed: 25838373]
5. Zou W, Wolchok JD, Chen L. PD-L1 (B7-H1) and PD-1 pathway blockade for cancer therapy: Mechanisms, response biomarkers, and combinations. Sci Transl Med. 2016; 8:328rv4.
6. Pitt JM, Vétizou M, Daillère R, et al. Resistance mechanisms to immune-checkpoint blockade in cancer: Tumor-intrinsic and -extrinsic factors. Immunity. 2016; 44:1255–69. [PubMed: 27332730]
7. Greten TF, Wang XW, Korangy F. Current concepts of immune based treatments for patients with HCC: from basic science to novel treatment approaches. Gut. 2015; 64:842–8. [PubMed: 25666193]
8. Kudo M. Immune checkpoint inhibition in hepatocellular carcinoma: basics and ongoing clinical trials. Oncology. 2017; 92(Suppl 1):50–62. [PubMed: 28147363]
9. Prieto J, Melero I, Sangro B. Immunological landscape and immunotherapy of hepatocellular carcinoma. Nat Rev Gastroenterol Hepatol. 2015; 12:681–700. [PubMed: 26484443]
10. Speiser DE, Ho P-C, Verdeil G. Regulatory circuits of T cell function in cancer. Nat Rev Immunol. 2016; 16:599–611. [PubMed: 27526640]
11. Gehring AJ, Ho ZZ, Tan AT, et al. Profile of Tumor Antigen-specific CD8 T cells in patients with hepatitis B virus-related hepatocellular Carcinoma. Gastroenterology. 2009; 137:682–90. [PubMed: 19394336]

12. Gabrielson A, Wu Y, Wang H, et al. Intratumoral CD3 and CD8 T-cell Densities Associated with Relapse-Free Survival in HCC. Cancer Immunol Res. 2016; 4:419–30. [PubMed: 26968206]
13. Tang H, Wang Y, Chlewicki LK, et al. Facilitating T Cell Infiltration in Tumor Microenvironment Overcomes Resistance to PD-L1 Blockade. Cancer Cell. 2016; 30:500. [PubMed: 27622338]
14. Ribas A, Hu-Lieskovan S. What does PD-L1 positive or negative mean? J Exp Med. 2016; 213:2835–40. [PubMed: 27903604]
15. Gabrilovich DI, Ostrand-Rosenberg S, Bronte V. Coordinated regulation of myeloid cells by tumours. Nat Rev Immunol. 2012; 12:253–68. [PubMed: 22437938]
16. Bronte V, Brandau S, Chen S-H, et al. Recommendations for myeloid-derived suppressor cell nomenclature and characterization standards. Nat Commun. 2016; 7:12150. [PubMed: 27381735]
17. Kalathil S, Lugade AA, Miller A, et al. Higher frequencies of GARP+CTLA-4+Foxp3+ T regulatory cells and myeloid-derived suppressor cells in hepatocellular carcinoma patients are associated with impaired T-cell functionality. Cancer Res. 2013; 73:2435–44. [PubMed: 23423978]
18. Hoechst B, Ormandy LA, Ballmaier M, et al. A new population of myeloid-derived suppressor Cells in hepatocellular carcinoma patients induces CD4+CD25+Foxp3+ T Cells. Gastroenterology. 2008; 135:234–43. [PubMed: 18485901]
19. Arihara F, Mizukoshi E, Kitahara M, et al. Increase in CD14+HLA-DR−/low myeloid-derived suppressor cells in hepatocellular carcinoma patients and its impact on prognosis. Cancer Immunology, Immunotherapy. 2013; 62:1421–30. [PubMed: 23764929]
20. Mizukoshi E, Yamashita T, Arai K, et al. Myeloid-derived suppressor cells correlate with patient outcomes in hepatic arterial infusion chemotherapy for hepatocellular carcinoma. Cancer Immunology, Immunotherapy. 2016; 65:715–25. [PubMed: 27083166]
21. Kapanadze T, Gamrekelashvili J, Ma C, et al. Regulation of accumulation and function of myeloid derived suppressor cells in different murine models of hepatocellular carcinoma. J Hepatol. 2013; 59:1007–13. [PubMed: 23796475]
22. Malumbres M, kinases C-dependent. Genome Biol. 2014; 15:122. [PubMed: 25180339]
23. O'Leary B, Finn RS, Turner NC. Treating cancer with selective CDK4/6 inhibitors. Nat Rev Clin Oncol. 2016; 13:417–30. [PubMed: 27030077]
24. Asghar U, Witkiewicz AK, Turner NC, et al. The history and future of targeting cyclin-dependent kinases in cancer therapy. Nat Rev Drug Discov. 2015; 14:130–46. [PubMed: 25633797]
25. Feng H, Cheng ASL, Tsang DP, et al. Cell cycle–related kinase is a direct androgen receptor–regulated gene that drives β-catenin/T cell factor–dependent hepatocarcinogenesis. J Clin Invest. 2011; 121:3159–75. [PubMed: 21747169]
26. Yu Z, Gao Y-Q, Feng H, et al. Cell cycle-related kinase mediates viral-host signalling to promote hepatitis B virus-associated hepatocarcinogenesis. Gut. 2014; 63:1793–804. [PubMed: 24440987]
27. Feng H, Yu Z, Tian Y, et al. A CCRK-EZH2 epigenetic circuitry drives hepatocarcinogenesis and associates with tumor recurrence and poor survival of patients. J Hepatol. 2015; 62:1100–11. [PubMed: 25500144]
28. Dorand RD, Nthale J, Myers JT, et al. Cdk5 disruption attenuates tumor PD-L1 expression and promotes antitumor immunity. Science. 2016; 353:399–403. [PubMed: 27463676]
29. Wells AD, Morawski PA. New roles for cyclin-dependent kinases in T cell biology: linking cell division and differentiation. Nat Rev Immunol. 2014; 14:261–70. [PubMed: 24603166]
30. Zhou J, Cheung AKL, Tan Z, et al. PD1-based DNA vaccine amplifies HIV-1 GAG-specific CD8+ T cells in mice. J Clin Invest. 2013; 123:2629–42. [PubMed: 23635778]
31. Cx L, Ling CC, Shao Y, et al. CXCL10/CXCR3 signaling mobilized-regulatory T cells promote liver tumor recurrence after transplantation. Journal of hepatology. 2016; 65:944–52. [PubMed: 27245433]
32. Goodwin TJ, Zhou Y, Musetti SN, et al. Local and transient gene expression primes the liver to resist cancer metastasis. Sci Transl Med. 2016; 364:ra153.
33. Tan Z, Zhou J, Cheung AKL, et al. Vaccine-elicited CD8+ T cells cure mesothelioma by overcoming Tumor-induced immunosuppressive environment. Cancer Res. 2014; 74:6010–21. [PubMed: 25125656]

34. Shin H-M, Kim M-H, Kim BH, et al. Inhibitory action of novel aromatic diamine compound on lipopolysaccharide-induced nuclear translocation of NF-κB without affecting IκB degradation. FEBS Lett. 2004; 571:50–4. [PubMed: 15280016]
35. Lee ST, Li Z, Wu Z, et al. Context-specific regulation of NF-κB target gene expression by EZH2 in breast cancers. Mol Cell. 2011; 43:798–810. [PubMed: 21884980]
36. De Henau O, Rausch M, Winkler D, et al. Overcoming resistance to checkpoint blockade therapy by targeting PI3Kγ in myeloid cells. Nature. 2016; 539:443–7. [PubMed: 27828943]
37. Kim K, Skora AD, Li Z, et al. Eradication of metastatic mouse cancers resistant to immune checkpoint blockade by suppression of myeloid-derived cells. Proc Natl Acad Sci U S A. 2014; 111:11774–9. [PubMed: 25071169]
38. Moynihan KD, Opel CF, Szeto GL, et al. Eradication of large established tumors in mice by combination immunotherapy that engages innate and adaptive immune responses. Nat Med. 2016; 22:1402–10. [PubMed: 27775706]
39. Awuah PK, Monga SP. Cell cycle-related kinase links androgen receptor and β-catenin signaling in hepatocellular carcinoma: Why are men at a loss? Hepatology. 2012; 55:970–4. [PubMed: 22362601]
40. Wang S-H, Yeh S-H, Chen P-J. The driving circuit of HBx and androgen receptor in HBV-related hepatocarcinogenesis. Gut. 2014; 63:1688–9. [PubMed: 24598130]
41. Naugler WE, Sakurai T, Kim S, et al. Gender disparity in liver cancer due to sex differences in MyD88-dependent IL-6 production. Science. 2007; 317:121–4. [PubMed: 17615358]
42. He G, Dhar D, Nakagawa H, et al. Identification of liver cancer progenitors whose malignant Progression depends on autocrine IL-6 signaling. Cell. 2013; 155:384–96. [PubMed: 24120137]
43. Lechner MG, Liebertz DJ, Epstein AL. Characterization of cytokine-induced myeloid-derived Suppressor cells from normal human peripheral blood mononuclear cells. The Journal of Immunology. 2010; 185:2273–84. [PubMed: 20644162]
44. Klein SL, Flanagan KL. Sex differences in immune responses. Nat Rev Immunol. 2016; 16:626–38. [PubMed: 27546235]
45. Spranger S, Bao R, Gajewski TF. Melanoma-intrinsic β-catenin signalling prevents antitumour immunity. Nature. 2015; 523:231–5. [PubMed: 25970248]
46. Peng D, Kryczek I, Nagarsheth N, et al. Epigenetic silencing of TH1-type chemokines shapes tumour immunity and immunotherapy. Nature. 2015; 527:249–53. [PubMed: 26503055]
47. Welte T, Kim IS, Tian L, et al. Oncogenic mTOR signalling recruits myeloid-derived suppressor cells to promote tumour initiation. Nat Cell Biol. 2016; 18:632–44. [PubMed: 27183469]
48. Sade-Feldman M, Kanterman J, Klieger Y, et al. Clinical significance of circulating CD33+CD11b +HLA-DR- myeloid cells in patients with stage IV melanoma treated with Ipilimumab. Clinical Cancer Research. 2016; 22:5661–72. [PubMed: 27178742]

Significance of this study

What is already known on this subject?

- Recent clinical trials have demonstrated that inhibition of immunoregulatory checkpoints such as the programmed death-1-ligand 1 (PD-L1)/programmed cell death receptor 1 axis, which elicits antitumour T cell responses in a broad spectrum of cancers, has produced durable efficacy in a fraction of patients with advanced hepatocellular carcinoma (HCC).
- The heterogeneous responses to immune-checkpoint blockade therapy are attributable to the complex interplay between a range of cancer cell autonomous cues and the tumour microenvironment, in particular through myeloid-derived suppressor cell (MDSC) immunosuppression.
- The latest cyclin-dependent kinase family member, cell cycle-related kinase (CCRK), is a new HCC oncogene that activates multiple protumorigenic signalling pathways.

What are the new findings?

- Concordant overexpression of CCRK, interleukin (IL) 6 and MDSC markers correlates with poor prognosis of patients with HCC.
- Tumour-intrinsic CCRK mitigates antitumour T cell responses by expanding MDSCs via an enhancer of zeste homolog 2/nuclear factor-κB/IL-6 cascade.
- Targeting tumorous Ccrk signalling diminishes MDSC-mediated immunosuppression to inhibit HCC tumorigenicity.
- Tumorous *Ccrk* depletion upregulates PD-L1 expression and increases intratumorous effector T cells, which improve anti-PD-L1 therapy for large hepatoma eradication.

How might it impact on clinical practice in the foreseeable future?

- These findings elucidate a novel therapeutic kinase target in HCC that shapes the immunosuppressive microenvironment to blunt antitumour immune responses.
- Our results suggest that co-blockade of CCRK and PD-L1 represents a rational development of combination immunotherapy for patients with HCC.

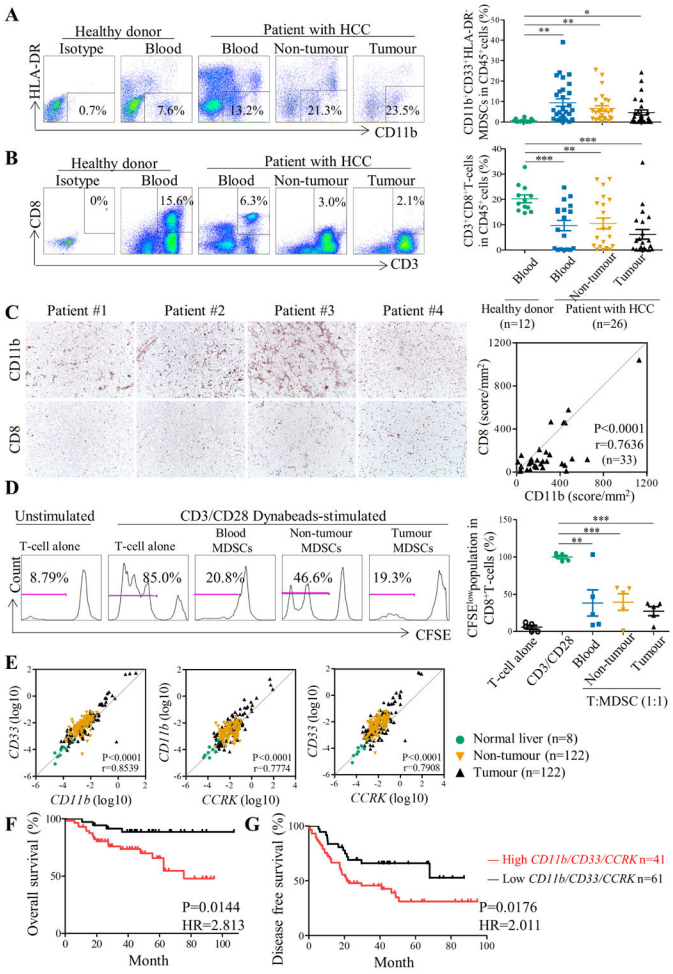

Figure 1.

Cell cycle-related kinase (CCRK) overexpression in human hepatocellular carcinomas (HCCs) correlates with immunosuppressive $CD11b^{+}CD33^{+}HLA\ DR^{-}$ myeloid-derived suppressor cell (MDSC) accumulation and poor patient survivals. (A) Representative $CD11b^{+}HLA\text{-}DR^{-}$ MDSCs dot plots are shown in blood, non-tumour and tumour tissues from patients with HCC and healthy controls following a leucocytes gate ($CD45^{+}$). Cells stained by isotype antibody were used as fluorescence baseline control. CD33 expression in $CD11b^{+}HLA\text{-}DR^{-}$ cells were further analysed and presented in 26 patients with HCC and 12 healthy donors. (B) Corresponding $CD3^{+}CD8^{+}$ T cell proportions in $CD45^{+}$ leucocytes were determined. *, p<0.05; **, p<0.01; ***, p<0.001. (C) Representative pictures of CD11b and CD8 immunohistochemical staining in tumours of patients with HCC are shown (x100 magnification). The association between CD11b and CD8 scores is shown in 33 patients with HCC. (D) Autologous T cell proliferation assay. The percentage of carboxyfluorescein succinimidyl ester $(CFSE)^{low}$ population represents the proportion of proliferating $CD3^{+}CD8^{+}$ T cells. Representative flow cytometry data and a statistical diagram are shown. (E) The mRNA level of MDSC markers *CD11b*, *CD33* and *CCRK* relative to *GAPDH* was measured by quantitative reverse transcription-PCR. Correlations among *CD11b*, *CD33* and *CCRK* in 122 HCC tumour and paired nontumour tissues as well as 8 normal liver tissues

were denoted with Pearson's correlation coefficients (**r**). (F) Kaplan-Meier overall survival and (G) disease-free survival curves of patients with HCC with high (n=41) and low (n=61) expressions (stratified by median) of *CD11b*, *CD33* and *CCRK* mRNAs.

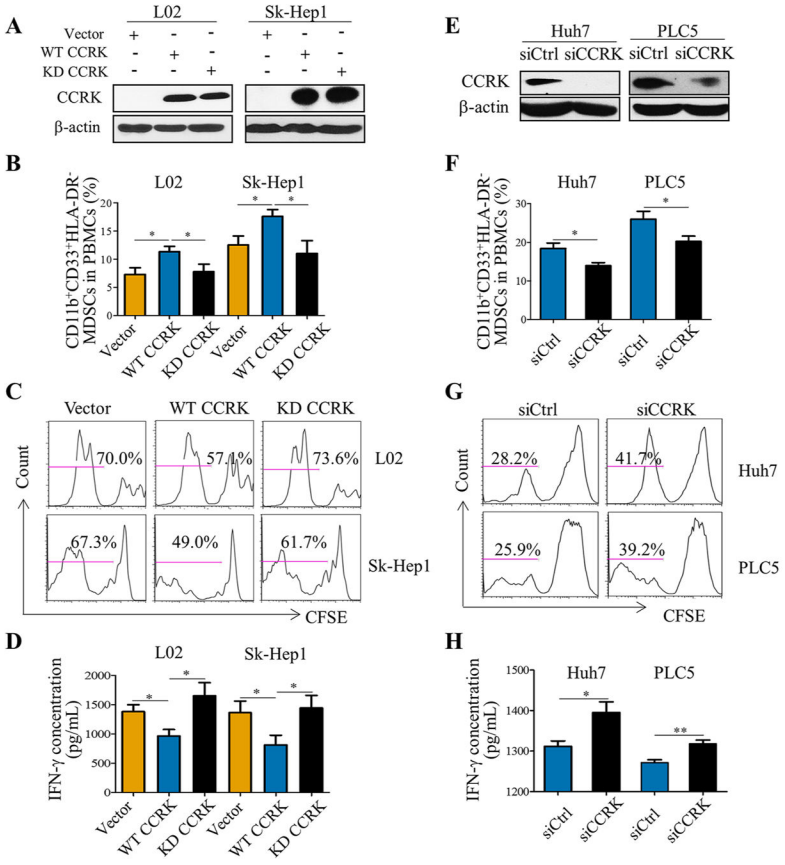

Figure 2.

Hepatocellular cell cycle-related kinase (CCRK) induces T cell-suppressive myeloid-derived suppressor cell (MDSC) expansion from human peripheral blood mononuclear cells (PBMCs). (A) Immunoblot analysis of CCRK in LO2 and Sk-Hep1 cells expressing wild type (WT) or kinase-defective (KD) CCRK compared with pcDNA3.1 vector control. β-actin was used as loading control. (B) The percentages of $CD11b^{+}CD33^{+}HLADR^{-}$ MDSCs in PMBCs treated with conditional medium from vector, WT or KD CCRK-expressing L02 and Sk-Hep1 cells. (C) The percentages of $CFSE^{low}$ proliferated $CD3^{+}$ T cells and (D) interferon γ (IFN-γ) production levels on co-culture with the stimulated PMBCs as described in (B) were presented by histogram and bar charts, respectively. (E) Immunoblot analysis in Huh7 and PLC5 cells with or without short-interfering RNA (siRNA)-mediated CCRK knockdown. (F) The percentages of $CD11b^{+}CD33^{+}HLA\text{-}DR^{-}$ MDSCs, (G) $CFSE^{low}$ proliferated $CD3^{+}$ T cells and (H) IFN-γ levels in the control and CCRK knockdown groups are shown. The data represent at least five independent experiments. *, $p<0.05$; **, $p<0.01$.

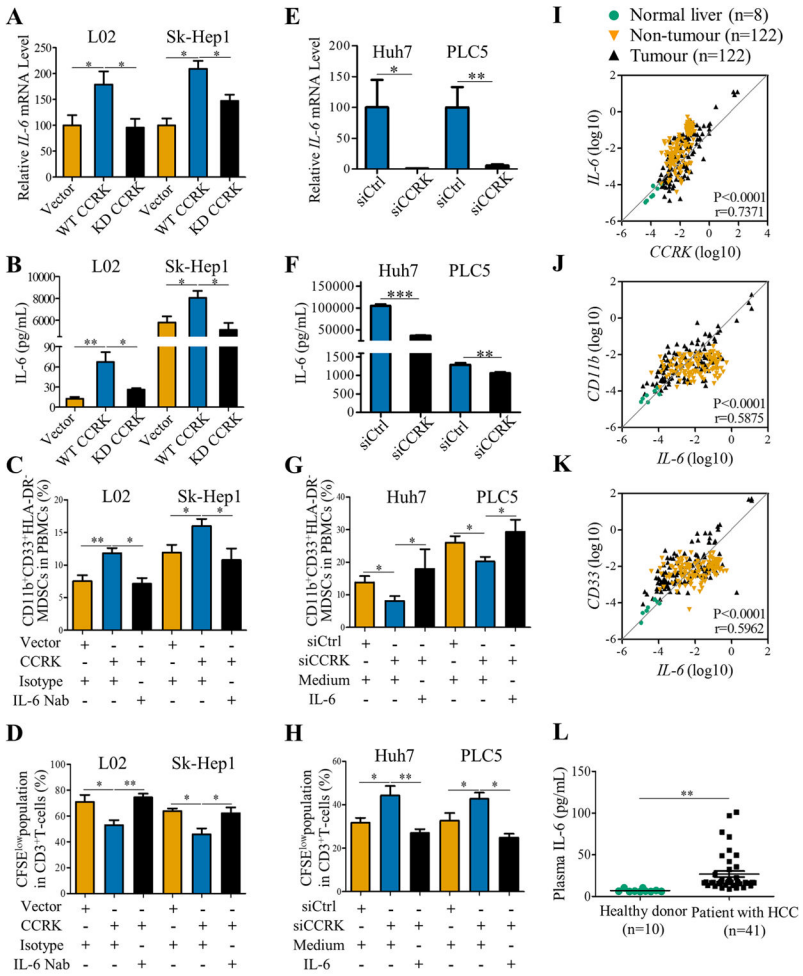

Figure 3.

Hepatocellular cell cycle-related kinase (CCRK) induces myeloid-derived suppressor cell (MDSC) expansion through IL-6 production. (A) Quantitative reverse transcription-PCR (qRT-PCR) and (B) ELISA analyses of *IL-6* mRNA and protein levels, respectively, in LO2 and Sk-Hep1 cells expressing wild type (WT) or kinase-defective (KD) CCRK compared with pcDNA3.1 vector control. The mRNA and supernatants were collected at 24 hours and 72 hours post-transfection, respectively. (C) The percentages of $CD11b^{+}CD33^{+}HLA\text{-}DR^{-}$ MDSCs in PMBCs treated with conditional medium from vector, WT CCRK-expressing L02 and Sk-Hep1 cells with or without IL-6 neutralisation antibody (Nab; 100 ng/mL). (D) The percentages of $CFSE^{low}$ proliferated $CD3^{+}$ T cells on co-culture with the stimulated PMBCs as described in (C) were presented in bar charts. (E) qRT-PCR and (F) ELISA analyses of *IL-6* mRNA and protein levels, respectively, in Huh7 and PLC5 cells with or without short-interfering RNA (siRNA)-mediated knockdown of CCRK. The mRNA and supernatants were collected at 24 hours and 72 hours post-transfection, respectively. (G) The percentages of $CD11b^{+}CD33^{+}HLA\text{-}DR^{-}$ MDSCs in PMBCs treated with conditional medium from CCRK-knockdown Huh7 and PLC5 cells with or without recombinant IL-6 protein (100 ng/mL). (H) The percentages of $CFSE^{low}$ proliferated $CD3^{+}$ T cells on co-culture with the stimulated PMBCs as described in (G) were presented in bar charts. The

data represent at least five independent experiments. (I–K) The *IL-6* mRNA level relative to *GAPDH* was measured by qRT-PCR. Correlations among (I) *IL-6* and *CCRK*, (J) *CD11b* and *IL-6*, and (K) *CD33* and *IL-6* in 122 hepatocellular carcinoma (HCC) tumour and paired non-tumour tissues as well as eight normal liver tissues were denoted with Pearson's correlation coefficients (**r**). (L) Serum IL-6 concentrations in 41 patients with HCC and 10 healthy donors were measured by ELISA. *, $p<0.05$; **, $p<0.01$.

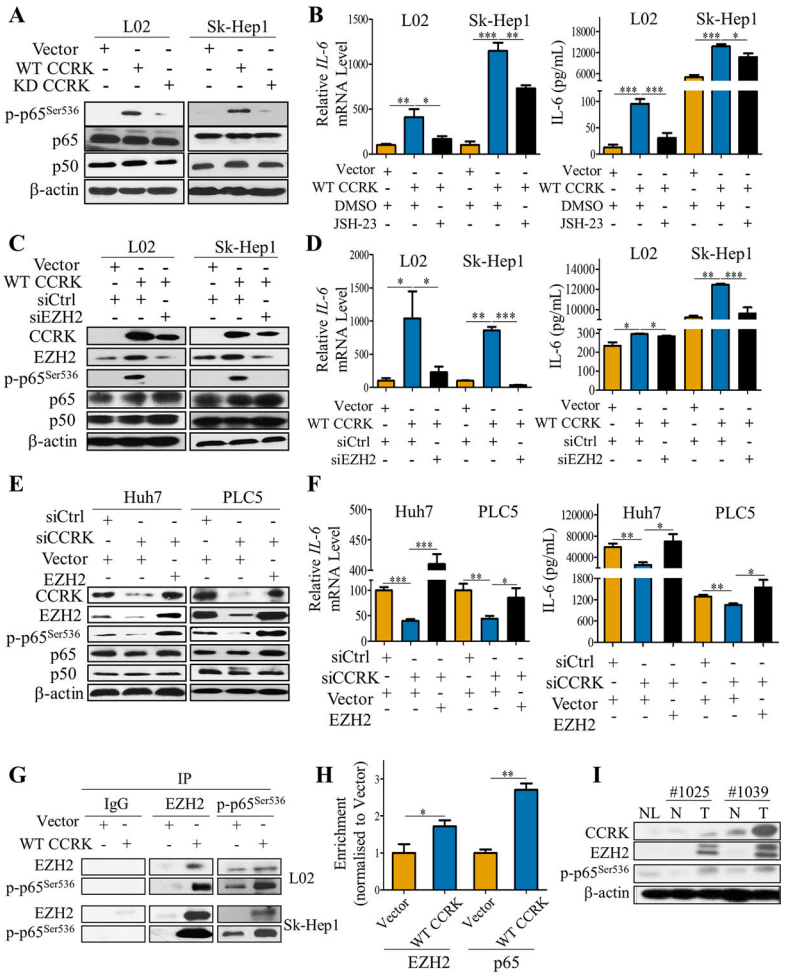

Figure 4.

Hepatocellular cell cycle-related kinase (CCRK) activates enhancer of zeste homologue 2 (EZH2)-nuclear factor-κB (NF-κB) signalling pathway to stimulate IL-6 production. (A) Immunoblot analysis of phosphorylated p65 (Ser536), p65 and p50 in LO2 and Sk-Hep1 cells expressing wild type (WT) or kinase-defective (KD) CCRK compared with pcDNA3.1 vector control. β-actin was used as loading control. (B) Quantitative reverse transcription-PCR (qRT-PCR) and ELISA analysis of *IL-6* mRNA and protein, respectively, in control or WT CCRK-expressing LO2 and Sk-Hep1 cells with or without treatment with JSH-23 (10 μM). (C) Immunoblot of CCRK, EZH2, phosphorylated p65 (Ser536), p65 and p50, (D) qRT-PCR and ELISA analyses of *IL-6* mRNA and protein, respectively, in control and WT CCRK-expressing LO2 and Sk-Hep1 cells with or without short-interfering RNA (siRNA)-mediated knockdown of EZH2. (E) Immunoblot of CCRK, EZH2, phosphorylated p65 (Ser536), p65 and p50, (F) qRT-PCR and ELISA analyses of *IL-6* mRNA and protein, respectively, in Huh7 and PLC5 cells co-transfected with siCtrl or siCCRK and EZH2 or empty vector. The data represent at least five independent experiments. (G) Co-immunoprecipitation(IP) of EZH2 and p-p65^{Ser536} in control and WT CCRK-expressing LO2 and Sk-Hep1 cells, followed by immunoblot analysis of EZH2 and p-p65^{Ser536}. IgG represents a control antibody used for IPs. (H) Quantitative chromatin immunoprecipitation-

PCR (qChIP-PCR) analyses of EZH2 and p65 on *IL-6* promoter in control and WT CCRK-expressing LO2 cells. The data represent at least three independent experiments. *, $p<0.05$; **, $p<0.01$; ***, $p<0.001$. (I) Representative immunoblot analysis of CCRK, EZH2 and p-$p65^{Ser536}$ in human normal liver (NL), matched non-tumour (N) and tumour (T) tissues from two patients with hepatocellular carcinoma (HCC). β-actin was used as loading control.

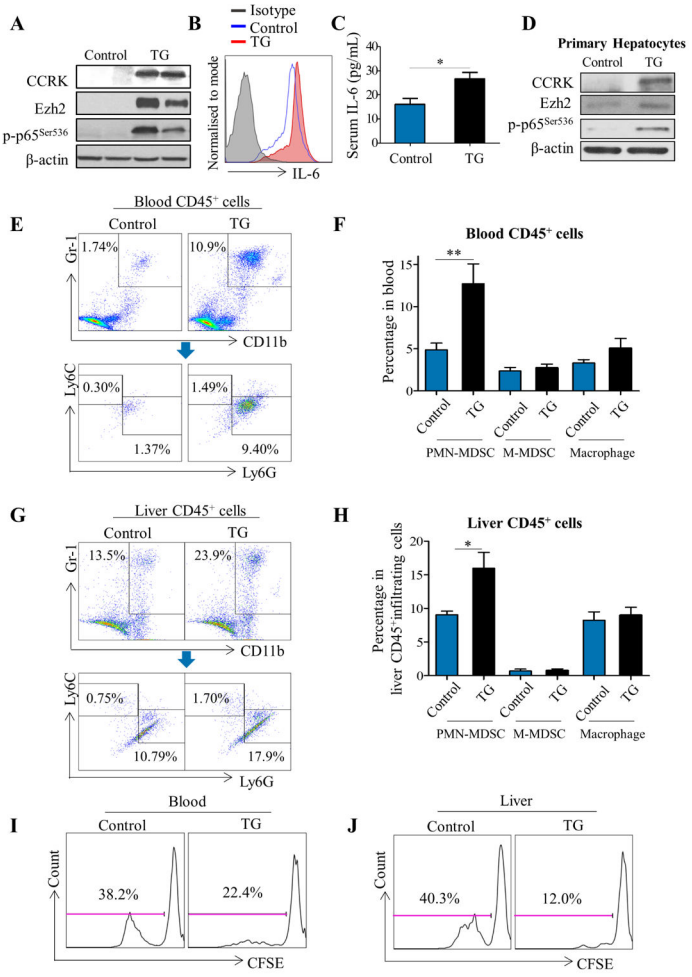

Figure 5.

Liver-specific cell cycle-related kinase (*CCRK)* expression selectively enhances polymorphonuclear (PMN)-myeloid-derived suppressor cell (MDSC) accumulation and T cell suppression in transgenic (TG) mice. (A) *CCRK* expression was induced by tamoxifen in transferrin promoter (*pTf)-LSL-CCRK/+, Rosa26CreERt2/+* (TG) mice. Immunoblot analysis of CCRK, enhancer of zeste homologue 2 (EZH2) and phosphorylated p65 (Ser536) in liver tissues harvested from *Rosa26CreERt2/+* (control) and *CCRK* TG mice at 10 days post-tamoxifen injection. β-actin was used as loading control. (B) IL-6 levels in $CD45^{-}$ liver cells and (c) serum of control and *CCRK* TG mice were determined by flow cytometry and ELISA, respectively. (D) Primary hepatocytes isolated from control and TG mice were infected by Cre-expressing adenovirus to induce CCRK expression. Immunoblot analysis of CCRK, EZH2 and phosphorylated p65 (Ser536) in hepatocytes at 4 days postinfection. (E) Representative flow cytometry dot plots of $CD11b^{+}Gr\text{-}1^{+}Ly6G^{+}Ly6C^{int}$PMN-MDSCs in control and TG mouse blood $CD45^{+}$ cells. (**F**) The proportions of PMN-MDSC, monocytic (M)-MDSC and macrophage were measured in peripheral blood mononuclear cells (PBMCs) isolated from male mouse blood at 30 days post-tamoxifen injection. (G) The representative flow cytometry dot plots of $CD11b^{+}Gr\text{-}1^{+}Ly6G^{+}Ly6C^{int}$PMN-MDSCs and (H) the myeloid cell proportions in the livers of control and TG mice are shown. The data

contain two independent sets of control and TG mice (n≥6). (I) $CD11b^{+}Gr\text{-}1^{+}Ly6G^{+}Ly6C^{int}$PMN-MDSCs were sorted from control and TG mice blood or (J) liver, followed by co-culture with CFSE-labelled splenic $CD3^{+}$ T cells from Balb/c mice at the ratio of 1:1 in the presence of phorbol 12-myristate 13-acetate (50 ng/mL) and ionomycin (500 ng/mL) for 3 days. $CFSE^{low}$ proportion in $CD3^{+}$ T cells was measured by flow cytometry (n≥3). *, $p<0.05$; **, $p<0.01$.

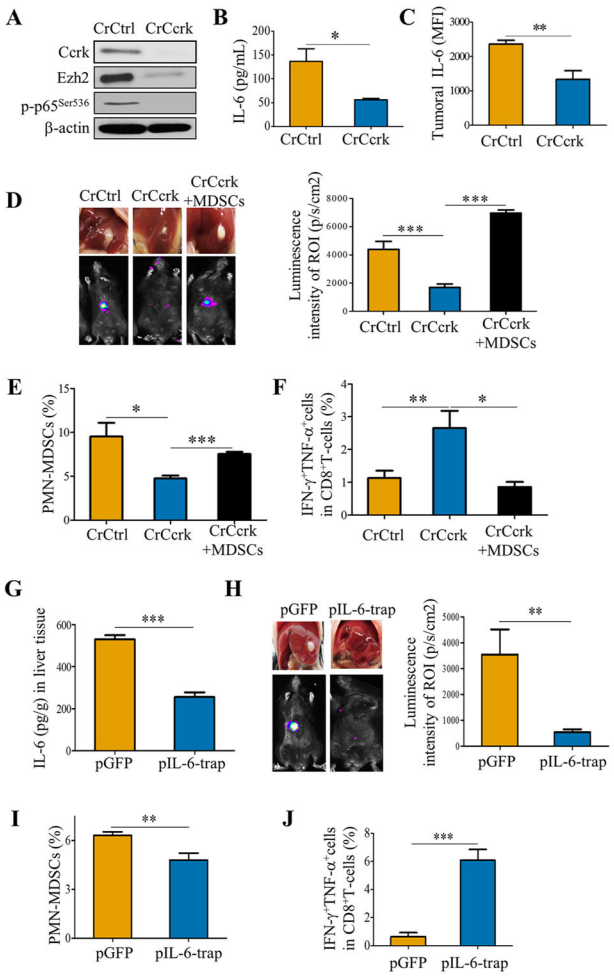

Figure 6.

Cell cycle-related kinase (Ccrk)/IL-6 signalling promotes tumour growth via inducing polymorphonuclear (PMN)-myeloid-derived suppressor cells (MDSCs) in orthotopic hepatocellular carcinoma (HCC) model. (A) Immunoblot of Ccrk, Ezh2, phosphorylated p65 (Ser536) and (B) ELISA analyses of IL-6 production in CRISPR/Cas9-derived control (CrCtrl) and *Ccrk*-depleted (CrCcrk) Hepa1–6 murine hepatoma cells. β-actin was used as loading control. (C) Tumorous IL-6 expression was determined by mean fluorescence intensity (MFI) of intracellular IL-6 in $CD45^{-}$ tumour cells. (D) Representative morphology and luciferase images of livers. The average tumour size determined by luminescence intensity of region of interest (ROI) in the three groups are shown. (E) The percentages of $CD11b^{+}Gr\text{-}1^{+}Ly6G^{+}Ly6C^{int}$ PMN-MDSCs and (F) Interferon γ (IFN-γ)$^{+}$ tumour necrosis factor (TNF)-α$^{+}CD8^{+}$ T cells in tumour-infiltrating $CD45^{+}$leucocytes were measured by flow cytometry. (G) Hepatic IL-6 depletion in the orthotopic HCC model using lipid/calcium/phosphate (LCP) nano particles encapsulating IL-6 protein trap (pIL-6-trap) or green fluorescent protein control (pGFP) control plasmid. ELISA analysis of IL-6 concentration in liver tissue lysates of the pGFP and pIL-6-trap groups. (H) Representative morphology and luciferase images of livers in both groups are shown. The average tumour size was determined by luminescence intensity of ROI. (I) The percentages of CD11b

$^{+}$Gr-1^{+}Ly6G^{+}Ly6C^{int} PMN-MDSCs and (J) IFN-γ^{+} TNF-α^{+}CD8^{+} T cells in tumour-infiltrating CD45^{+} leucocytes were measured by flow cytometry. *, $p<0.05$; **, $p<0.01$; ***, $p<0.001$.

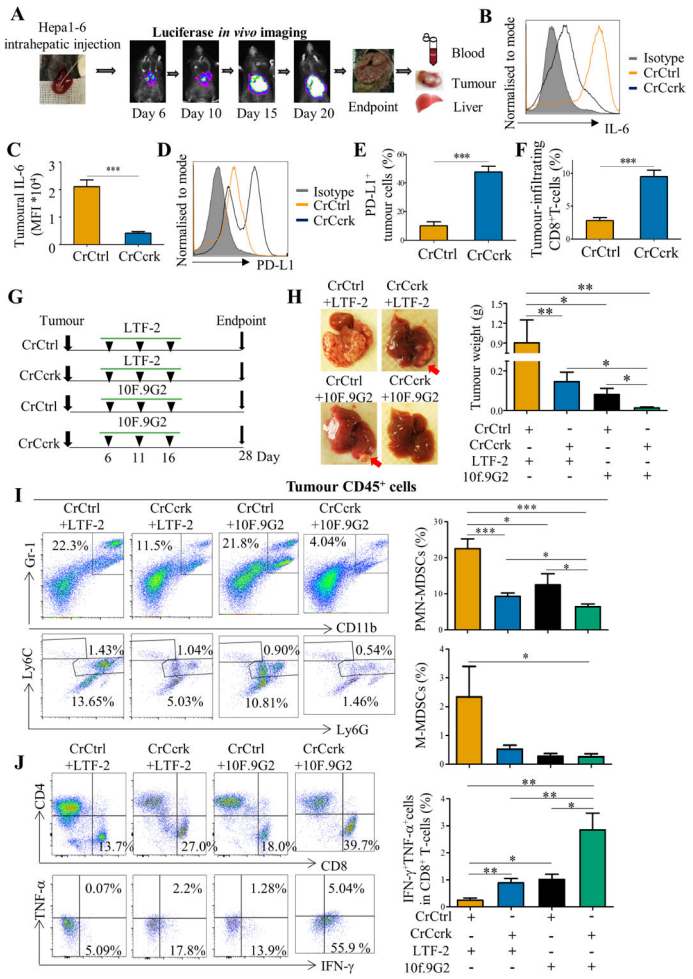

Figure 7.

Inhibition of tumorous cell cycle-related kinase (*Ccrk)* enhances the efficacy of antiprogrammed death-1-ligand-1 (PD-L1) therapy to eradicate large hepatoma. (A) Schematic diagram of the orthotopic hepatocellular carcinoma (HCC) model via direct intrahepatic Hepa1-6 cell injection, generating large hepatoma in vivo. (B) IL-6 levels of $CD45^{-}$CrCtrl and CrCcrk tumour cells were determined by flow cytometry and (C) depicted as maximum fluorescence intensity (MFI) in the bar chart. (D) PD-L1 expressions on $CD45^{-}$CrCtrl and CrCcrk tumour cells were determined by flow cytometry and (E) depicted as percentage of $PD\text{-}L1^{+}$ tumour cells in the bar chart. (F) The proportions of $CD8^{+}$ T cells in tumour-infiltrating $CD45^{+}$ leucocytes were measured by flow cytometry. (G) Single or combined blockade of *Ccrk* and PD-L1 in the large hepatoma model using CrCtrl or CrCcrk Hepa1-6 cells and rat IgG2b control (LTF-2) or anti-PD-L1 antibody (10F.9G2), respectively. The antibodies were intraperitoneally injected (200 μg/each) at 6 days, 11 days and 16 days post-tumour cell intrahepatic injection. Mice were sacrificed after 28 days for blood/liver/tumour sample collections (n>6 per group). (H) Representative images of livers in the four groups are shown. The average tumour weight was determined. (**I**) Representative flow cytometry dot plots and the percentages of $CD11b^{+}Gr\text{-}1^{+}Ly6G^{+}Ly6C^{int}$ polymorphonuclear (PMN)-myeloid-derived suppressor cells (MDSCs), $CD11b^{+}Gr\text{-}1^{+}Ly6G$

$^{-}$Ly6C^{+} monocytic (M)-MDSCs and (**J**) Interferon γ (IFN-γ)$^{+}$ tumour necrosis factor (TNF)-α^{+}CD8^{+} T cells in tumourinfiltrating CD45^{+} cells were measured (n≥6). CrCtrl, *Ccrk* control. *, p<0.05; **, p<0.01; ***, p<0.001.

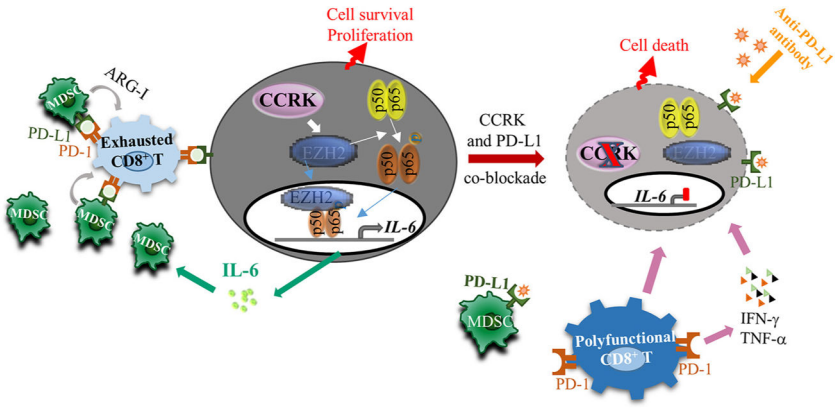

Figure 8.

Schematic representation of the hepatoma-intrinsic cell cycle-related kinase (CCRK) signalling in hepatocellular carcinoma (HCC) immune evasion. Therapeutic co-blockade of *CCRK* and programmed death-1-ligand 1 (PD-L1) would simultaneously inhibit myeloid-derived suppressor cell (MDSC) accumulation and engender polyfunctional $CD8^+$ T cell responses in the tumour environment, resulting in eradication of HCC. ARG-I, arginase-I; EZH2, enhancer of zeste homologue 2; IFN-γ, interferon γ; PD-1, programmed cell death receptor 1; TNF-α, tumour necrosis factor α.